HHS Public Access

Author manuscript

Genes Chromosomes Cancer. Author manuscript; available in PMC 2019 October 01.

Published in final edited form as:

Genes Chromosomes Cancer. 2018 October ; 57(10): 485–494. doi:10.1002/gcc.22643.

Comparative Analysis of *AKT* and the related biomarkers in uterine leiomyomas with *MED12*, *HMGA2* and *FH* mutations

Jia Xie[1], **Julianne Ubango**[1], **Yanli Ban**[1], **Debabrata Chakravarti**[2], **J. Julie Kim**[2], and **Jian-Jun Wei**[1,2,*]

[1]Department of Pathology, Feinberg School of Medicine, Northwestern University, Chicago, IL, USA

[2]Department of Obstetrics and Gynecology, Feinberg School of Medicine, Northwestern University, Chicago, IL, USA

Abstract

Uterine leiomyomas (ULM) are histologically and molecularly heterogeneous and clinically they grow at vastly different rates. Several driver gene mutations have been identified in ULM, including *MED12* mutations, *HMGA2* overexpression, and biallelic FH inactivation. ULM with different driver mutant genes may use different molecular pathways, but currently no clear correlation between gene mutations and growth related pathways has been established. To better define this relationship, we collected ULM with *MED12* (n=25), *HMGA2* (n=15) and *FH* (n=27) mutations and examined the sex steroid hormone, cell cycle, and AKT pathway genes by immunohistochemistry. While ER and PR were highly expressed in all types of ULM, *FH* ULM showed lower *ER* expression and higher *PR* expression. *HMGA2* tumors had significantly higher levels of AKT signaling and mitogenic activity than other ULM types. *HMGA2* activated AKT signaling through upregulation of IGFB2P. Silencing *HMGA2* in ULM cells resulted in downregulation of AKT and upregulation of p16 and p21, which eventually led to cell senescence. *HMGA2* overexpression in ULM is not only related to tumor development but also plays a role in controlling cellular proliferation through the AKT pathway.

Keywords

Leiomyoma; mutations; *HMGA2*; *MED12*; *FH*; pathway analysis; cellular senescence

1. Introduction

Uterine leiomyomas (ULM) are an important public health problem due to the high incidence among women and the high rate of surgical intervention with myomectomy or hysterectomy[1]. Up to 70% of women develop ULM during their lifetime[2] and current medical therapies show no significant long term benefits, but carry significant side effects. ULM are a histologically and molecularly heterogeneous group of tumors and grow at vastly

*Corresponding Author: Jian-Jun Wei, M.D., Department of Pathology,, Robert H. Lurie Comprehensive Cancer Center, Northwestern University, Feinberg School of Medicine, 251 East Huron Street, Feinberg 7-334, Chicago, Illinois 60611, Phone:312-926-1815, Fax: 312-926-3127, jianjun-wei@northwestern.edu.

different rates.[3] Yet the pathogenesis of ULM leading to the varied histology and growth behavior is largely unknown. In recent studies, several driver gene mutations have been identified in ULM, including *MED12* mutations in exon 2 in 60-70% of cases, *HMGA2* overexpression in 10-15% of cases, and biallelic *FH* inactivation in rare cases[4, 5]. Global gene expression analysis indicates that different mutant genes in ULM may target different molecular pathways[5] and each mutation type may theoretically determine growth behavior, but these theories have not yet been proven. Notably, a uterus with multiple ULM can show somatic mutations of different genes and each given tumor only acquires a single driver gene mutation, since the mutations are mutually exclusive[4, 6, 7]. Thus, ULM consist of a group of genetically heterogeneous tumors with similar histogenesis.

Such genetic differences in ULM due to different driver gene mutations may determine their histological and molecular heterogeneity and further influence tumor growth rates. However, histology and molecular pathway correlation with these driver gene mutations has not been established or characterized. *HMGA2* overexpression in ULM is caused by a translocation between 12q and 14q[8] and the early studies showed that ULM with *HMGA2* overexpression tend to be larger and grow faster than those without *HMGA2* alterations[5, 9, 10]. *HMGA2* ULM cannot be differentiated histologically from other ULM, but it is common in a variant of ULM defined as intravascular leiomyomatosis[11]. Unfortunately, while many oncogenic functions of *HMGA2* in malignant tumors are characterized[12], little is known about how *HMGA2* causes and promotes ULM development and growth. *MED12* mutations are the most common somatic mutations in ULM[13]. MED12 is essential for activating CDK8 and modulates mediator-polymerase II interactions for transcription initiation[14]. Growth of *MED12* ULM may require and recruitment of prominent myoma-associated fibroblasts[15]. *FH* ULM exhibit characteristic histologic features in leiomyomas of bizarre nuclei[16, 17]. Further investigation of the molecular and histological difference in ULM with different driver gene mutations may assist in understanding biological and medical significance and aid in clinical management.

Since sex steroid hormones, cell cycle and AKT signaling are prevalent pathways for ULM growth, we aimed in this study to examine these common functional pathways in ULM with different driver mutations. We collected ULM with *MED12*, *HMGA2* and *FH* mutations and examined the selected markers by immunohistochemistry. The functional correlation between AKT and *HMGA2* was further analyzed in primary cultures of ULM.

2. MATERIALS AND METHODS

2.1 Case selection

Human myometrial and leiomyoma tissues were collected from premenopausal women undergoing hysterectomy at the Northwestern University. The use of human tissue specimens was approved by the Institutional Review Board for Human Research at Northwestern University. Fresh frozen and/or formalin-fixed and paraffin-embedded tumor, and myometrial tissues were used. The genotypes of the selected ULM with MED12 mutations, HMGA2 overexpression and biallelic FH inactivation have been reported in previous studies[6, 16].

2.2 Primary cell culture for ULM

Subjects were only included in the study if they were not taking hormonal contraceptives or gonadotropin-releasing hormone agonists/antagonists for at least 3 months. Informed consent was obtained from all the patients participating in the study. After tissue was collected, primary myometrial and leiomyoma cells were isolated and cultured. Primary cells were cultivated in Dulbecco's modified Eagle's medium/nutrient Ham's Mixture F-12 (DMEM-F12) 1:1 containing 10% fetal bovine serum (FBS) and 1% penicillin-streptomycin at 37°C and 5% CO_2 atmosphere. Primary ULM cell cultures were maintained in Smooth Muscle Growth Medium-2 (SmGM™-2 medium) (Lonza) to avoid loss of myoma cells.

2.3 Senescence-associated β-galactosidase (SA-β-gal) staining

The cells were treated with MK2206 at 5μM (Merck Sharp & Dohme Corp.) Then the cells were fixed with 2% formaldehyde plus 0.2% glutaraldehyde and were stained with β-galactosidase staining solution (citric acid/sodium phosphate solution, potassium ferrocyanide, potassium ferricyanide, X-gal, pH6). They were incubated at 37°C overnight in a dry incubator and the reactions were terminated when the cells were stained blue-green, as visualized under an inverted bright-field microscope. The cells were also stained with DAPI (4′, 6-Diamidino-2-Phenylindole, Dihydrochloride) to show the nucleus. Three images were taken randomly under each treatment condition and then the percentage of the cells that were positive for β-galactosidase was calculated.

2.4 SDS-PAGE and Western blotting

Protein lysates were extracted from myometrial and leiomyoma cells using RIPA lysis and extraction buffer with protease and phosphatase inhibitors (Thermo Fisher Scientific). The protein concentration was determined using BCA Protein Assay kit (Thermo Fisher Scientific). Equal amounts of proteins were subjected to SDS-PAGE and subsequently transferred to polyvinylidene difluoride (PVDF) membranes. Immunoblotting was performed using the following primary antibodies: p21 Waf1/Cip1 (12D1) Rabbit mAb (Cell Signaling Technology), Human p16INK4a/CDKN2A Antibody (Fisher Scientific), pAKT and AKT (Cell Signaling Technology), HMGA2 (Biocheck Inc), and β-actin Antibody (Cell Signaling Technology). Secondary antibodies were horseradish peroxidase (HRP)-labeled anti-mouse (7076S, Cell Signaling Technology), anti-rabbit (7074S, Cell Signaling Technology), or anti-goat (HAF109, Fisher Scientific). Chemiluminescence was detected by adding a chemiluminescent HRP substrate (Thermo Fisher Scientific) and measured with a Fujifilm LAS-3000 Imager.

2.5 RNA isolation and RT-PCR

RNA was isolated from uterine fibroid cells using Rneasy Mini Kit (Qiagen) and reverse-transcribed with M-MLV Reverse Transcriptase (Clontech) following the manufacturer's instructions. Quantitative RT-PCR was performed using PowerUp™ SYBR® Green Master Mix (Life Technologies) on an Applied Biosystems® Real-Time PCR Instrument. *HMGA2* primers were: Forward 5′-TCCGGTGTTGATGGTGGCAG-3′; Reverse 5′-CTTGGCCGTTTTTCTCCAGTG-3′. GAPDH was used as the housekeeping gene, and

relative mRNA levels were calculated using the $2^{-\Delta\Delta Ct}$ method. Each data point is the average of three replicates.

2.6 *HMGA2* siRNA Transient Transfection

Cells were grown to 60%-80% confluency at the day of transfection, and then were either transfected with control siRNA (Stealth RNAi negative control duplexes, ThermoFisher Scientific) or HMGA2 siRNA (Stealth siRNA, HSS111974, ThermoFisher Scientific) according to the manufacturer's instruction using Lipofectamine RNAiMAX (ThermoFisher Scientific), as described previously in detail[12].

2.7 Tissue microarrays

Formalin-fixed paraffin-embedded (FFPE) tissue blocks with the most accurate morphological features were selected for each case and 2 mm^2 tissue cores were taken to create tissue microarrays (TMAs). The TMAs were sectioned at 4 μm. The first and last slides were stained with hematoxylin and eosin (H&E) for quality assurance to confirm the correct tumor types and the presence of viable tumor tissue.

2.8 Immunohistochemistry

The analytical markers for immunohistochemical (IHC) analysis included steroid hormone receptors (ER and PR), cell cycle marker (p16), and cell proliferative marker (Ki-67), and AKT pathway markers (pAKT, pS6, IGF2BP2). The driver gene markers of FH, HMGA2 and MED12 were also included in examining the selected cases. All immunohistochemical staining procedures were performed on a Ventana Nexus automated system as described previously[6]. All information regarding selected antibodies is summarized in Supplementary Table 1. The percent and intensity of each staining were evaluated by two pathologists. The intensity was scored as negative (0), weak (1+), moderate (2+), or strong (3+) and the percentage of positive tumor cells was scored from 0% to 100%. The results were then semi-quantitatively analyzed.

2.9 Statistical analysis

GraphPad Prism software was used for statistical analysis and IHC data were presented as median and ranges for the entire tumor samples and the control myometrium. Other data were presented as mean and standard deviation. Student's t-test or one way Anova analysis was used to determine statistical significance. A p value less than 0.05 was considered statistically significant.

3. RESULTS

3.1 Selection of ULM with *MED12*, *HMGA2* and *FH* mutations

Previously, 178 ULM cases were tested for mutational analysis of *MED12* and *HMGA2*[6]. *MED12* exon 2 mutations were detected by Sanger sequencing and *HMGA2* overexpression was identified by immunohistochemistry. *MED12* mutations were found in 75.4% (134/178) ULM, *HMGA2* overexpression in 10.1% of the cases (18/178). We also examined FH expression by immunohistochemistry and loss of *FH* expression was detected in 1.1% of the

cases (2/178). In all 178 cases, the three gene mutations were mutually exclusive. After genotype was determined by gene mutation analysis (*MED12* exon 2) and immunohistochemistry (*HMGA2* overexpression and loss of *FH*), the cases from each of three gene mutations were selected for this study. We then selected 25 ULM with *MED12* mutations, and 15 ULM with *HMGA2* overexpression for this study. We also selected 27 ULM with loss of *FH* in our collection of leiomyoma with bizarre nuclei[16]. Histologically, *MED12* ULM showed varied cellularity of smooth muscle cells with prominent extracellular matrix and low vasculature (Figure 1; H/E). *HMGA2* ULM presented with increased cellularity[4] and vasculature. *FH* ULM have their characteristic large and small round/oval nuclei, prominent nucleoli and dilated vessels (Figure 1). The demographic information for our patients is summarized in Table 1. The tumor size and patient age differed significantly among the three gene mutations. Patients with *FH* ULM were significantly younger than those with *MED12* and *HMGA2* ULM and *HMGA2* ULM had significantly larger tumors than the other two.

3.2 Sex steroid hormone expression in different types of ULM

The relative expression of ER and PR were scored semi-quantitatively using percentage and intensity of staining. In all myometrial controls, ER and PR expression was high with a median score of 70% (95% of CI in 58-74%; Table 2). Overall, ULM also showed high levels of ER and PR expression with a range of 45-80% staining. No significant difference between myometrial controls and ULM was noted. When ER and PR expression was reviewed based on different gene mutations, *FH* ULM had significantly lower ER expression (45%) and bordering higher PR expression (84%) than both the other ULM subtypes and the myometrial controls ($p=0.0049$, $p=0.058$, respectively, Table 2, Figure 2). In fact, over 25% of *FH* ULM showed no ER expression (Figure 2A). In contrast, *HMGA2* and *MED12* ULM showed no significant difference in ER or PR expression and no difference when compared with myometrial controls ($p>0.05$). Similar trends were noted when comparing the staining intensity of ER and PR among the three variants (Table 2). These findings suggest that two of the molecular ULM subtypes maintain high levels of ER and PR expression. In contrast, the inverse association of ER and PR expression in *FH* ULM is noted with underlying mechanisms yet to be characterized.

3.3 Expression analysis of p16 and Ki-67

P16 is a major cell cycle regulator. In malignant tumors including leiomyosarcoma, diffuse p16 expression reflects loss of function due to an RB defect in the negative feedback loop[18]. In normal or benign tumors like nevi and ULM, p16 expression serves as a cell cycle inhibitor driving cells into senescence[19, 20]. In order to determine whether different driver gene mutations influenced tumor growth and arrest through p16, IHC staining for p16 was done in ULM. Overall ULM showed very low levels of p16 expression ranging from 1-5% p16 immunoreactivity. *HMGA2* ULM had almost undetectable p16 expression (0-3%) in comparison to *MED12* ULM (4.5-12.3%) and *FH* ULM (4.9-17.1%), which was statistically significant ($p<0.05\%$, Table 2, Figure 2C). This finding also correlated with a much higher proliferation index (Ki67) ranging from 5.6-14% in *HMGA2* ULM in comparison to 2.0-4.5% in *MED12* ULM and 0.2-2.4% in *FH* ULM ($p<0.05$, Figure 2D, Table 2). These

findings suggest that *HMGA2* promotes leiomyoma growth through its negative regulation of p16 expression.

3.4 Expression analysis of AKT pathway

AKT has been found to be activated in ULM and promotes fibroid growth and survival within an unfavorable hypoxic microenvironment[21]. AKT activation in ULM is not fully understood but we have demonstrated its association with the ROS pathway[22]. Here, we examined the levels of activated AKT and its direct downstream target, pS6, in ULM with the three different gene mutations. *HMGA2* ULM showed strong, diffuse immunoreactivity for pAKT and pS6. In contrast, weak to moderate immunoreactivity for pAKT and pS6 was present in *MED12* and *FH* ULM as well as in the myometrial controls (Figure 3, Table 2).

Previous gene profiling studies have shown that ULM with *HMGA2* overexpression have increased IGF2BP2 expression[5]. To test whether IGF2BP2 is a major upstream mediator for IGF2, we examined IGF2BP2 levels by immunohistochemistry. As illustrated in Figure 3B and 3C, almost all *HMGA2* ULM showed strong and diffuse immunoreactivity for IGF2BP2. In contrast, the other two subtypes and the myometrial controls showed low levels of IGF2BP2 ($p<0.001$). These findings suggest that an important interaction of IGF2BP2 and AKT occur in specifically *HMGA2* ULM.

3.5 Molecular analysis of *HMGA2*-mediated AKT signaling in ULM

The immunohistochemistry results suggest that ULM with *HMGA2* overexpression have significantly higher proliferation index, higher AKT activity, and lower p16 expression than the other two genetic subtypes. Thus, primary leiomyoma cells were used to evaluate the role of *HMGA2* in modulating AKT, p16 and p21. ULM with *MED12* mutations (low *HMGA2* levels) were used to overexpress *HMGA2* using lentiviral transduction using two MOIs, low (0.5) and moderate (1.0). A dose-dependent upregulation of pAKT was observed by Western blot analysis along with an increase in *HMGA2* levels (Figure 4A). Next, using *HMGA2* ULM, *HMGA2* was silenced using siRNA. With decreased *HMGA2* levels, decreased pAKT levels were observed (Figure 4B, C, and D). These data demonstrate the ability of *HMGA2* to regulate AKT activity. To evaluate whether AKT regulates *HMGA2* levels in ULM, AKT was blocked by the AKT inhibitor MK2206 and no significant change of *HMGA2* expression was noted (Figure 4E). These data support that *HMGA2* upregulates AKT and not the reverse.

3.6 Downregulation of *HMGA2* expression in primary culture fibroid cells leads to cellular senescence

We observed that serial passaging of primary culture leiomyoma cells led to profound replicative senescence and concurrent upregulation of both p16 and p21 (Jia et al, unpublished data). To evaluate the role of *HMGA2* in this process, primary ULM and matched myometrial (MM) cells were collected at P0, P1 (passage 1) and P2 (passage 2) and then *HMGA2* expression was examined by real-time quantitative RT-PCR (Figure 5A). While MM cells exhibited low expression of *HMGA2*, ULM cells at P0 had higher expression of *HMGA2*. In contrast, ULM at P1 and P2 exhibited decreased expression of *HMGA2* suggesting that *HMGA2* downregulation is correlated with replicative senescence.

To confirm that downregulation of *HMGA2* in primary culture of fibroid cells was the major driving force for cellular senescence, P0 cells were transfected with *HMGA2* siRNA and cellular senescence was examined by a β-Gal stain. As shown in Figure 5B, cells treated with *HMGA2* siRNA had significantly increased levels of β-Gal staining, indicative of cellular senescence than the cells treated with control siRNA (53% vs. 38%, $p<0.05$). Similar effects were observed when we used ELISA to measure β-Gal activity (Figure 5C). In addition, we observed in Figure 5D that silencing of *HMGA2* in ULM led to upregulation of both p16 and p21. Our findings suggest that the aggressive behavior of *HMGA2* ULM is due to increased tumor cell growth and survival through *HMGA2*, an enhanced AKT pathway and decreased cell cycle control. In contrast, when *HMGA2* is low, this leads to reduced AKT activity, increased cell cycle inhibition resulting in cellular arrest or senescence.

4. Discussion

ULM are sex steroid hormone driven tumors, characterized by fast growth rate during reproductive age. In general, most ULM, regardless of their underlying genetic mutations, express high levels of ER and PR (Figure 2). Our study has suggested that *HMGA2* ULM are a variant that tends to be larger and faster-growing than other genetic subtypes, indicating that this specific gene mutation may play a significant role in tumor growth on top of sex steroid hormone signaling. Therefore, non-hormonal pathways could be a major alternative drug target for fibroid treatment. In this study, we compared the selected cell cycle regulators and AKT in ULM with three different driver gene mutations and found that only the *HMGA2* tumors had high AKT activity, high cell proliferation indices (Ki-67), and significantly lower p16 expression (Figure 2).

HMGA2 mutations are the second most common driver mutations in ULM, accounting for 10-15% of the cases[6]. *HMGA2* ULM tend to be larger and faster-growing tumors in comparison to *MED12* and *FH* subtypes (Table 1)[5, 9, 10]. *HMGA2* is a transcriptional regulator and is highly associated with many functions, such as tumorigenesis, stem cell renewal, cell proliferation and cellular senescence. The function of *HMGA2* heavily relies on the cell type. For example, in ovarian and other cancer cells, *HMGA2* is an oncogene and promotes aggressive tumor growth through its multiple oncogenic properties[23]. In normal or benign tumor cells, it can promote cell proliferation and sensitizes to stress and oncogene-induced senescence[24]. *HMGA2* ULM are a subset of tumors which do not share the same major pathways as the other genetic subtypes and previous studies have demonstrated that repression of *HMGA2* by let-7 and other mechanisms resulted in decreased tumor growth[25]. Additionally, *HMGA2* ULM are larger and have higher rate of cell proliferation, supporting *HMGA2* as a mitogenic factor. Transgenic mouse models indicated that *HMGA2* can sufficiently repress p16 expression for stem cell self-renewal[26]. Since AKT pathway is one of the major pathways that regulates ULM growth[22, 27–29], *HMGA2* regulation of the AKT pathway is a significant discovery for ULM.

It has been shown that decreased *HMGA2* expression in acute myeloid leukemia cells inhibited cell proliferation through a decrease in the protein expression of pAKT and p-mTOR[30]. *HMGA2* may also directly regulate IGF2BP2 to influence IGF2 bioavailability in

other cell types[5, 31]. IGF2 is one of the major growth factors highly overexpressed in ULM[32]. We previously reported that IGF2 is overexpressed in ULM at the transcriptional level without changing IGF2 imprinting status in ULM[33]. Given that *HMGA2* may enhance IGF2 through IGF2BP2, we postulated that *HMGA2* overexpression can activate the AKT pathway in ULM and we indeed found that ULM with *HMGA2* overexpression showed a significant positive correlation with IGF2BP2, pAKT and pS6 overexpression (Figure 3). This finding was further validated by using *in vitro* primary leiomyoma cells (Figure 4). The results of our study provide further evidence that ULM with *HMGA2* overexpression can enhance AKT activity for tumor growth and survival.

In addition to promoting cell proliferation, *HMGA2* is also a major player in cellular senescence either under oncogenic[24] or environmental[29] stress. Several recent studies have shown that *HMGA2* regulates cell cycle genes. Silencing of *HMGA2* leads to the induction of cell cycle inhibitors, including cyclin D1, cyclin B1, and cyclin E expression and increases the number of cells in G0/G1 phase[34–36]. Interestingly, in our current study, we found that *HMGA2* expression was inversely proportional to p16 expression (Figure 2). When *HMGA2* was silenced in leiomyoma cells, it also resulted in the upregulation of p16 and p21 (Figure 5), leading to reduced tumor growth and increased cellular senescence (Figure 5). Based on this study, *HMGA2*-mediated AKT signaling and its regulation to cell proliferation and senescence in ULM is summarized in Figure 6.

Overall, we have shown that ULM with different driver gene mutations harbor different molecular pathways in regulating cell growth in ULM. These differences are reflected by their different growth rates and responses to environmental stress. Thus, *HMGA2* ULM are a group of tumors that could be treated differently from other ULM. In contrast, growth of *MED12* ULM may rely on tumor associated fibroblasts[15]. Therefore, with a better characterization of specific targets in ULM with different driver gene mutations, cell growth could be halted and cellular senescence could be induced in a more specific way. Moreover, gene mutation analysis in myomectomy specimen may help to predict the potential tumor growth and guide further clinical management when *HMGA2* overexpression is detected.

Supplementary Material

Refer to Web version on PubMed Central for supplementary material.

Acknowledgments

We would like to thank Mrs. Stacy Ann Kujawa for obtaining consents from patients and providing fresh samples for the study. All immunohistochemistry staining was performed in the Pathology Core Facility. This study was supported by NIH P01HD57877.

References

1. Farquhar CM, Steiner CA. Hysterectomy rates in the United States 1990–1997. Obstet Gynecol. 2002; 99:229–34. [PubMed: 11814502]
2. Baird DD, Dunson DB, Hill MC, Cousins D, Schectman JM. High cumulative incidence of uterine leiomyoma in black and white women: ultrasound evidence. Am J Obstet Gynecol. 2003; 188:100–7. [PubMed: 12548202]

3. Peddada SD, Laughlin SK, Miner K, Guyon JP, Haneke K, Vahdat HL, Semelka RC, Kowalik A, Armao D, Davis B, Baird DD. Growth of uterine leiomyomata among premenopausal black and white women. Proc Natl Acad Sci U S A. 2008; 105:19887–92. [PubMed: 19047643]
4. Makinen N, Kampjarvi K, Frizzell N, Butzow R, Vahteristo P. Characterization of MED12, HMGA2, and FH alterations reveals molecular variability in uterine smooth muscle tumors. Mol Cancer. 2017; 16:101. [PubMed: 28592321]
5. Mehine M, Kaasinen E, Heinonen HR, Makinen N, Kampjarvi K, Sarvilinna N, Aavikko M, Vaharautio A, Pasanen A, Butzow R, Heikinheimo O, Sjoberg J, Pitkanen E, Vahteristo P, Aaltonen LA. Integrated data analysis reveals uterine leiomyoma subtypes with distinct driver pathways and biomarkers. Proc Natl Acad Sci U S A. 2016; 113:1315–20. [PubMed: 26787895]
6. Bertsch E, Qiang W, Zhang Q, Espona-Fiedler M, Druschitz S, Liu Y, Mittal K, Kong B, Kurita T, Wei JJ. MED12 and HMGA2 mutations: two independent genetic events in uterine leiomyoma and leiomyosarcoma. Mod Pathol. 2014; 27:1144–53. [PubMed: 24390224]
7. Kampjarvi K, Makinen N, Mehine M, Valipakka S, Uimari O, Pitkanen E, Heinonen HR, Heikkinen T, Tolvanen J, Ahtikoski A, Frizzell N, Sarvilinna N, Sjoberg J, Butzow R, Aaltonen LA, Vahteristo P. MED12 mutations and FH inactivation are mutually exclusive in uterine leiomyomas. Br J Cancer. 2016; 114:1405–11. [PubMed: 27187686]
8. Hennig Y, Rogalla P, Wanschura S, Frey G, Deichert U, Bartnitzke S, Bullerdiek J. HMGIC expressed in a uterine leiomyoma with a deletion of the long arm of chromosome 7 along with a 12q14-15 rearrangement but not in tumors showing del(7) as the sole cytogenetic abnormality. Cancer Genet Cytogenet. 1997; 96:129–33. [PubMed: 9216720]
9. Wang T, Zhang X, Obijuru L, Laser J, Aris V, Lee P, Mittal K, Soteropoulos P, Wei J-J. A micro-RNA signature associated with race, tumor size, and target gene activity in human uterine leiomyomas. Genes Chromosomes and Cancer. 2007; 46:336–47. [PubMed: 17243163]
10. Quade BJ, Weremowicz S, Neskey DM, Vanni R, Ladd C, Dal Cin P, Morton CC. Fusion transcripts involving HMGA2 are not a common molecular mechanism in uterine leiomyomata with rearrangements in 12q15. Cancer Res. 2003; 63:1351–8. [PubMed: 12649198]
11. Ordulu Z, Nucci MR, Dal Cin P, Hollowell ML, Otis CN, Hornick JL, Park PJ, Kim TM, Quade BJ, Morton CC. Intravenous leiomyomatosis: an unusual intermediate between benign and malignant uterine smooth muscle tumors. Mod Pathol. 2016; 29:500–10. [PubMed: 26892441]
12. Wu J, Liu Z, Shao C, Gong Y, Hernando E, Lee P, Narita M, Muller W, Liu J, Wei JJ. HMGA2 overexpression-induced ovarian surface epithelial transformation is mediated through regulation of EMT genes. Cancer Res. 2011; 71:349–59. [PubMed: 21224353]
13. Makinen N, Mehine M, Tolvanen J, Kaasinen E, Li Y, Lehtonen HJ, Gentile M, Yan J, Enge M, Taipale M, Aavikko M, Katainen R, Virolainen E, Bohling T, Koski TA, Launonen V, Sjoberg J, Taipale J, Vahteristo P, Aaltonen LA. MED12, the mediator complex subunit 12 gene, is mutated at high frequency in uterine leiomyomas. Science. 2011; 334:252–5. [PubMed: 21868628]
14. Knuesel MT, Meyer KD, Donner AJ, Espinosa JM, Taatjes DJ. The human CDK8 subcomplex is a histone kinase that requires Med12 for activity and can function independently of mediator. Mol Cell Biol. 2009; 29:650–61. [PubMed: 19047373]
15. Wu X, Serna VA, Thomas J, Qiang W, Blumenfeld ML, Kurita T. Subtype-Specific Tumor-Associated Fibroblasts Contribute to the Pathogenesis of Uterine Leiomyoma. Cancer Res. 2017; 77:6891–901. [PubMed: 29055020]
16. Zhang Q, Poropatich K, Ubago J, Xie J, Xu X, Frizzell N, Kim J, Kong B, Wei JJ. Fumarate Hydratase Mutations and Alterations in Leiomyoma With Bizarre Nuclei. Int J Gynecol Pathol. 2017
17. Miettinen M, Felisiak-Golabek A, Wasag B, Chmara M, Wang Z, Butzow R, Lasota J. Fumarase-deficient Uterine Leiomyomas: An Immunohistochemical, Molecular Genetic, and Clinicopathologic Study of 86 Cases. Am J Surg Pathol. 2016; 40:1661–9. [PubMed: 27454940]
18. O'Neill CJ, McBride HA, Connolly LE, McCluggage WG. Uterine leiomyosarcomas are characterized by high p16, p53 and MIB1 expression in comparison with usual leiomyomas, leiomyoma variants and smooth muscle tumours of uncertain malignant potential. Histopathology. 2007; 50:851–8. [PubMed: 17543074]

19. Laser J, Lee P, Wei JJ. Cellular senescence in usual type uterine leiomyoma. Fertil Steril. 2010; 93:2020–6. [PubMed: 19217096]
20. Gray-Schopfer VC, Cheong SC, Chong H, Chow J, Moss T, Abdel-Malek ZA, Marais R, Wynford-Thomas D, Bennett DC. Cellular senescence in naevi and immortalisation in melanoma: a role for p16? Br J Cancer. 2006; 95:496–505. [PubMed: 16880792]
21. Hoekstra AV, Sefton EC, Berry E, Lu Z, Hardt J, Marsh E, Yin P, Clardy J, Chakravarti D, Bulun S, Kim JJ. Progestins activate the AKT pathway in leiomyoma cells and promote survival. J Clin Endocrinol Metab. 2009; 94:1768–74. [PubMed: 19240153]
22. Vidimar V, Gius D, Chakravarti D, Bulun SE, Wei JJ, Kim JJ. Dysfunctional MnSOD leads to redox dysregulation and activation of prosurvival AKT signaling in uterine leiomyomas. Sci Adv. 2016; 2:e1601132. [PubMed: 27847869]
23. Wu J, Wei JJ. HMGA2 and high-grade serous ovarian carcinoma. J Mol Med (Berl). 2013
24. Narita M, Narita M, Krizhanovsky V, Nunez S, Chicas A, Hearn SA, Myers MP, Lowe SW. A novel role for high-mobility group a proteins in cellular senescence and heterochromatin formation. Cell. 2006; 126:503–14. [PubMed: 16901784]
25. Peng Y, Laser J, Shi G, Mittal K, Melamed J, Lee P, Wei JJ. Antiproliferative effects by Let-7 repression of high-mobility group A2 in uterine leiomyoma. Mol Cancer Res. 2008; 6:663–73. [PubMed: 18403645]
26. Nishino J, Kim I, Chada K, Morrison SJ. Hmga2 promotes neural stem cell self-renewal in young but not old mice by reducing p16Ink4a and p19Arf Expression. Cell. 2008; 135:227–39. [PubMed: 18957199]
27. Dhingra S, Rodriguez ME, Shen Q, Duan X, Stanton ML, Chen L, Zhang R, Brown RE. Constitutive activation with overexpression of the mTORC2-phospholipase D1 pathway in uterine leiomyosarcoma and STUMP: morphoproteomic analysis with therapeutic implications. International journal of clinical and experimental pathology. 2011; 4:134–46.
28. Sefton EC, Qiang W, Serna V, Kurita T, Wei JJ, Chakravarti D, Kim JJ. MK-2206, an AKT Inhibitor, Promotes Caspase-Independent Cell Death and Inhibits Leiomyoma Growth. Endocrinology. 2013
29. Xu X, Lu Z, Qiang W, Vidimar V, Kong B, Kim JJ, Wei JJ. Inactivation of AKT induces cellular senescence in uterine leiomyoma. Endocrinology. 2014; 155:1510–9. [PubMed: 24476133]
30. Tan L, Wei X, Zheng L, Zeng J, Liu H, Yang S, Tan H. Amplified HMGA2 promotes cell growth by regulating Akt pathway in AML. J Cancer Res Clin Oncol. 2016; 142:389–99. [PubMed: 26319392]
31. Li Z, Zhang Y, Ramanujan K, Ma Y, Kirsch DG, Glass DJ. Oncogenic NRAS, required for pathogenesis of embryonic rhabdomyosarcoma, relies upon the HMGA2-IGF2BP2 pathway. Cancer Res. 2013; 73:3041–50. [PubMed: 23536553]
32. Wei JJ, Chiriboga L, Arslan AA, Melamed J, Yee H, Mittal K. Ethnic differences in expression of the dysregulated proteins in uterine leiomyomata. Hum Reprod. 2006; 21:57–67. [PubMed: 16172143]
33. Peng L, Wen Y, Han Y, Wei A, Shi G, Mizuguchi M, Lee P, Hernando E, Mittal K, et al. Expression of insulin-like growth factors (IGFs) and IGF signaling: molecular complexity in uterine leiomyomas. Fertility and Sterility. 2009; 91:2664–75. [PubMed: 18439583]
34. Xie H, Wang J, Jiang L, Geng C, Li Q, Mei D, Zhao L, Cao J. ROS-dependent HMGA2 upregulation mediates Cd-induced proliferation in MRC-5 cells. Toxicol In Vitro. 2016; 34:146–52. [PubMed: 27071802]
35. Esmailzadeh S, Mansoori B, Mohammadi A, Shanehbandi D, Baradaran B. siRNA-Mediated Silencing of HMGA2 Induces Apoptosis and Cell Cycle Arrest in Human Colorectal Carcinoma. J Gastrointest Cancer. 2017; 48:156–63. [PubMed: 27629422]
36. Li Y, Peng L, Seto E. Histone Deacetylase 10 Regulates the Cell Cycle G2/M Phase Transition via a Novel Let-7-HMGA2-Cyclin A2 Pathway. Mol Cell Biol. 2015; 35:3547–65. [PubMed: 26240284]

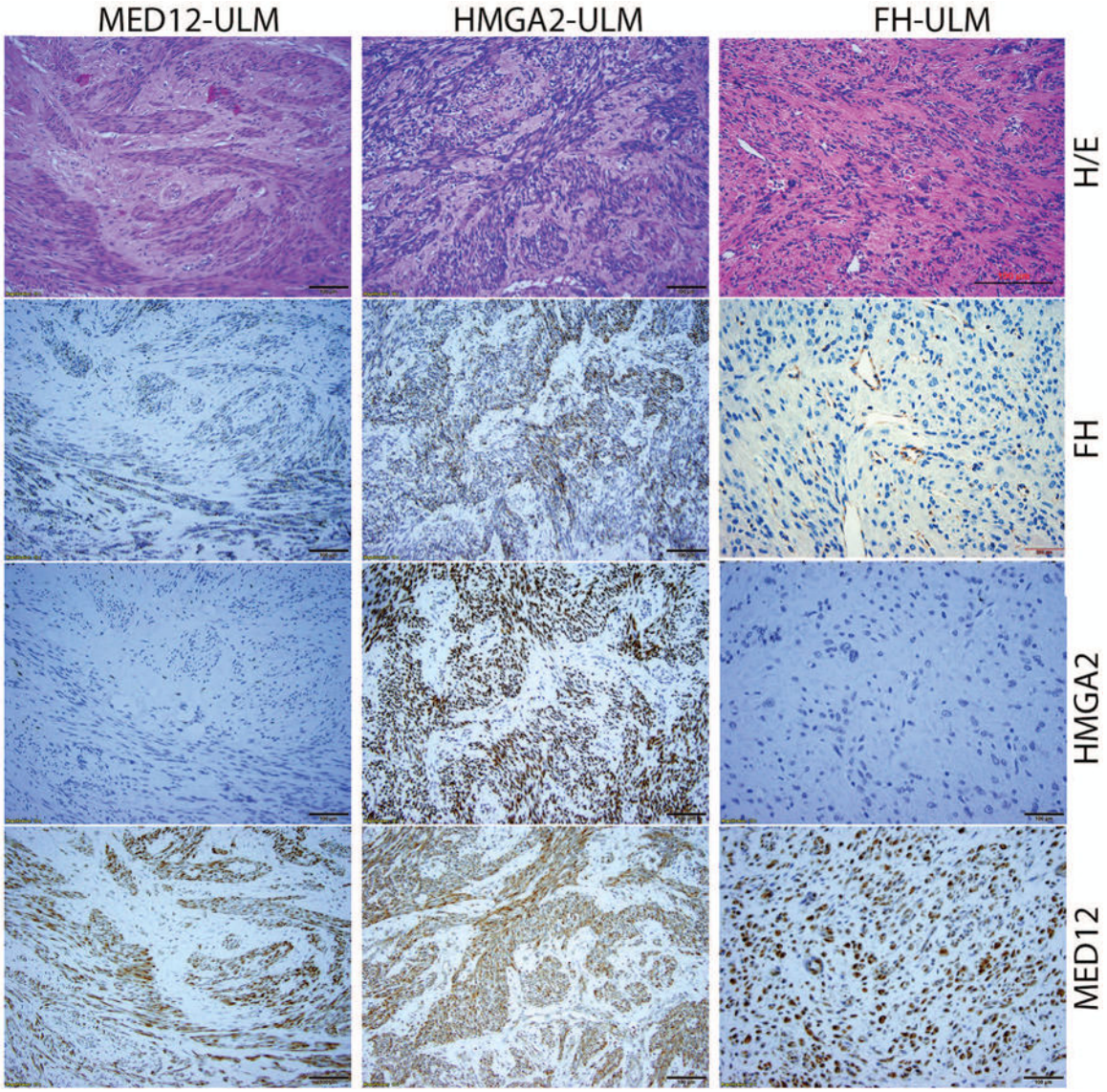

Figure 1.

Photomicrographs illustrate examples of ULM with *MED12* (*MED12*-ULM), *HMGA2* (*HMGA2*-ULM) and *FH* (*FH*-ULM) mutation/alteration. Tumor sections were examined by histology (H/E) and immunohistochemistry for *FH*, *HMGA2* and *MED12* (amplification ×20).

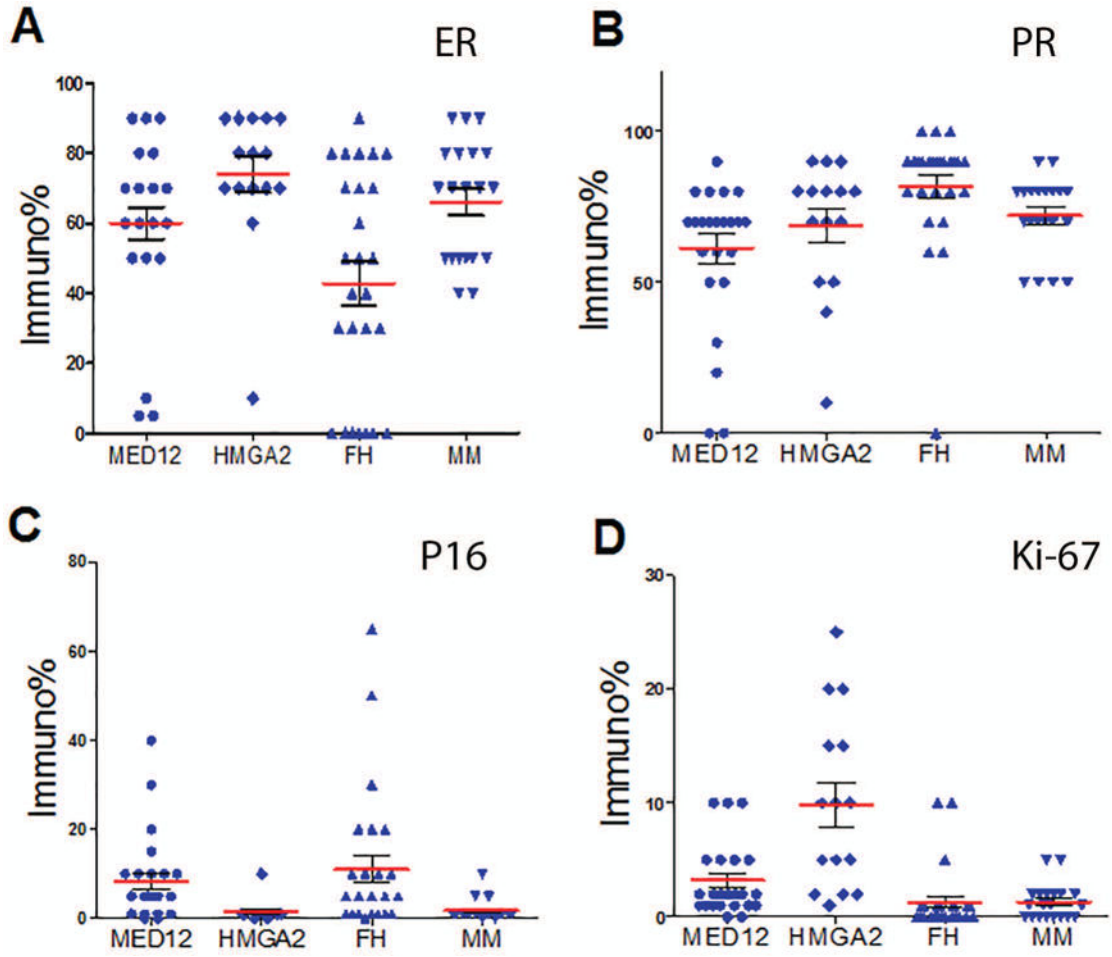

Figure 2.

Expression analysis of ER, PR, P16 and Ki-67 by immunohistochemistry in ULM with three different driver gene mutations/alteration. Dot plot illustration of estrogen receptor (ER, A), progesterone receptor (PR, B), P16 (C) Ki-67 (D) expression by immunopercentage in ULM with *MED12* mutation (rounded dot), HMGA2 overexpression (diagonal dot), loss of fumarate hydratase (FH) (upward triangle dot) and myometrium (downward triangle dot). Mean expression levels (Red line) and standard errors (short black line) for each tumor type are shown.

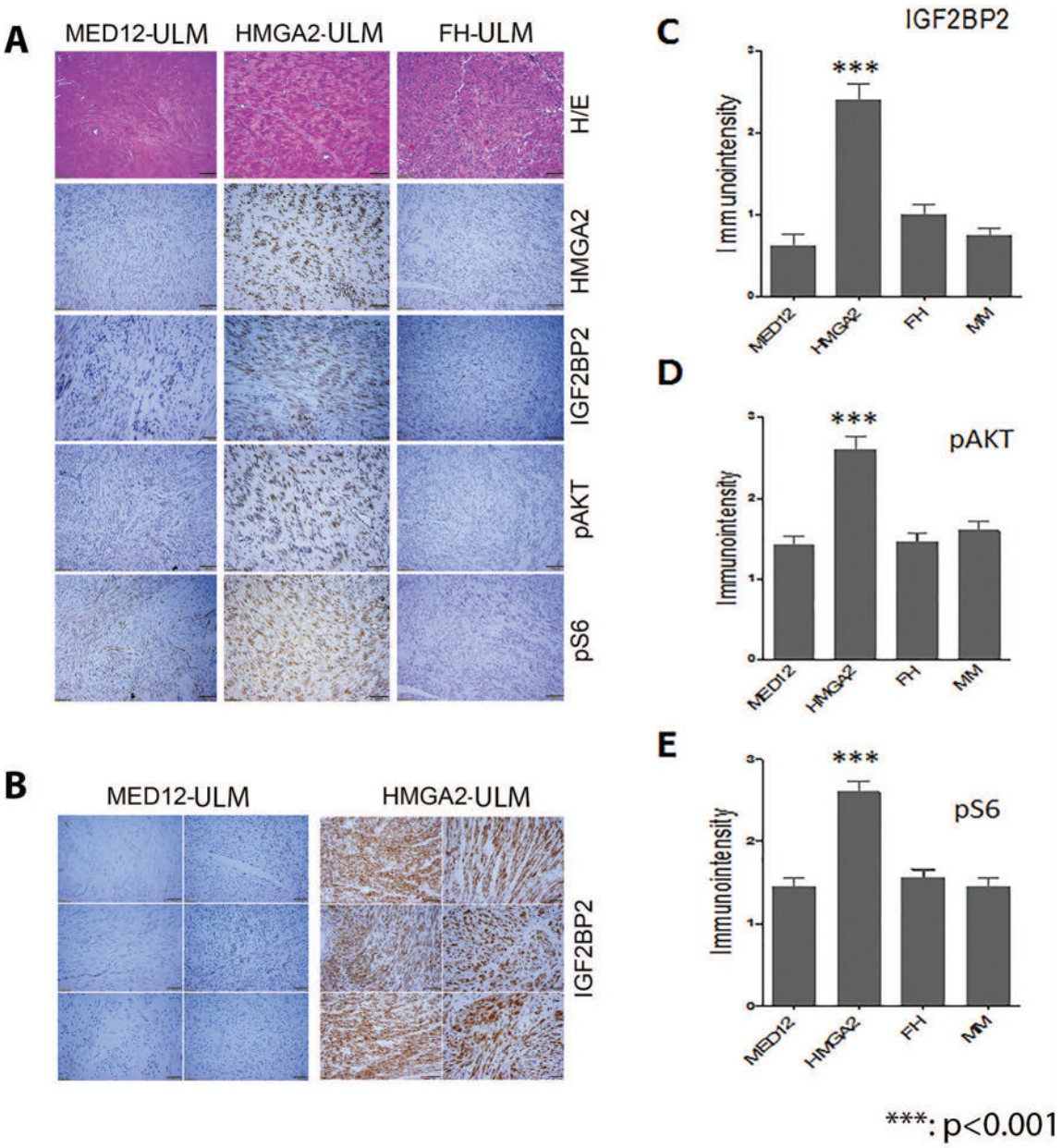

Figure 3.

Immunohistochemistry analysis of the selected biomarkers in AKT pathways in ULM with three different driver gene mutations/alteration. A. Photomicrographs illustrate examples of tumor sections of H/E and immunostaining (in the order of HMGA2, IGF2BP2, pAKT, and pS6,) slides for ULM with three different driver gene mutations. B. Closer view of immunoreactivity for IGF2BP2 in 6 HMGA2 (right) and 6 MED12 (left) ULM. C-E. Histobar analysis of IGF2BP (C), pAKT (D) pS6 (E) expression by immuno-intensity in ULM with different driver gene mutations and myometrium (MM).

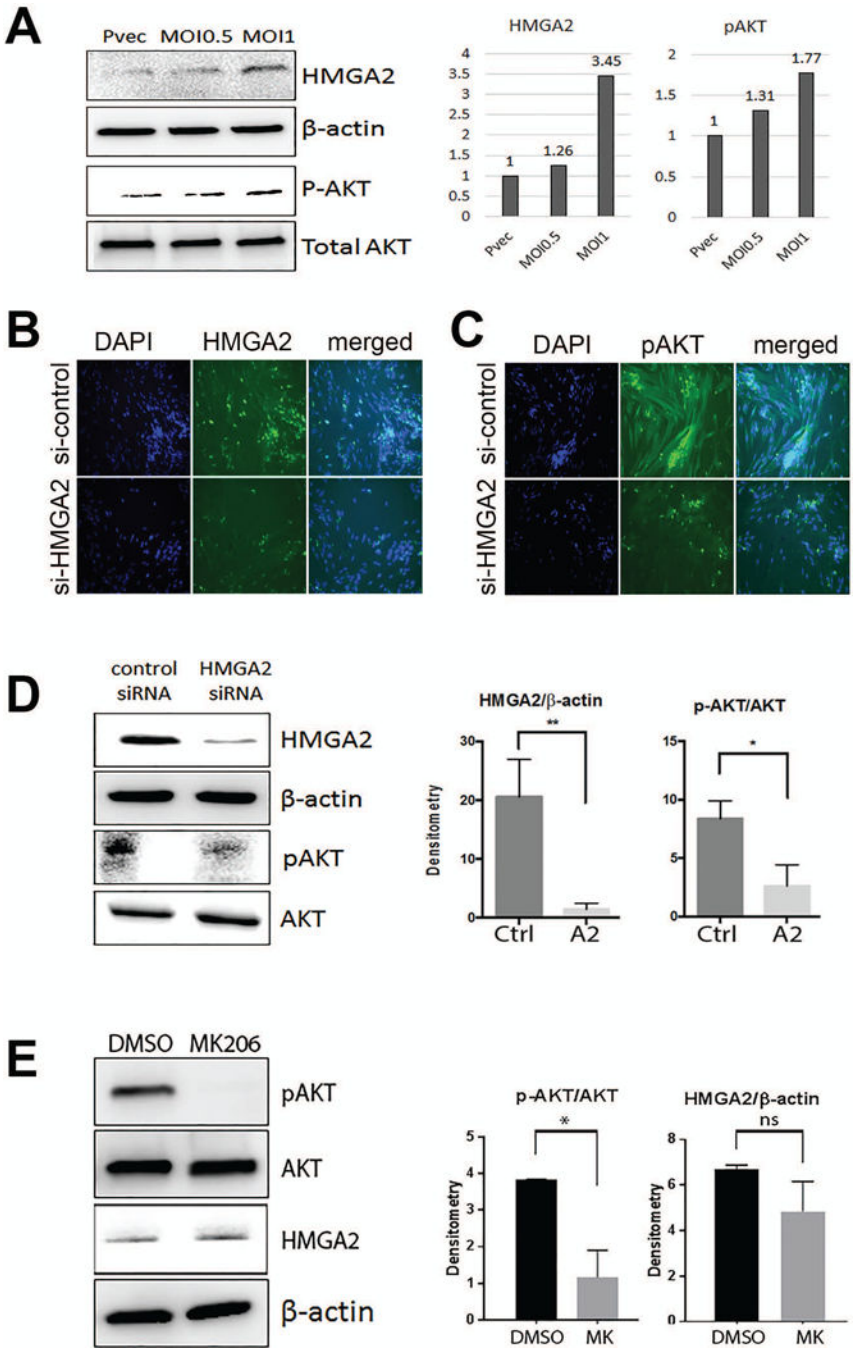

Figure 4.

Expression analysis of HMGA2 mediated AKT alteration in primary ULM cells. A. Overexpression of HMGA2 by lentiviral transduction increases pAKT activity in a dose dependent manner. B. and C. Decreased HMGA2 expression by siRNA was evident by immunofluorescent stain of *HMGA2* (B) and down regulation of pAKT occurs as a consequence (C). D. Western blot analysis illustrated that siRNA HMGA2 treatment significantly reduced pAKT, but not total AKT. E. Blocking pAKT activity by AKT inhibitor MK2206 showed minimal effect on HMGA2 expression. * $p<0.05$, ** $p<0.01$.

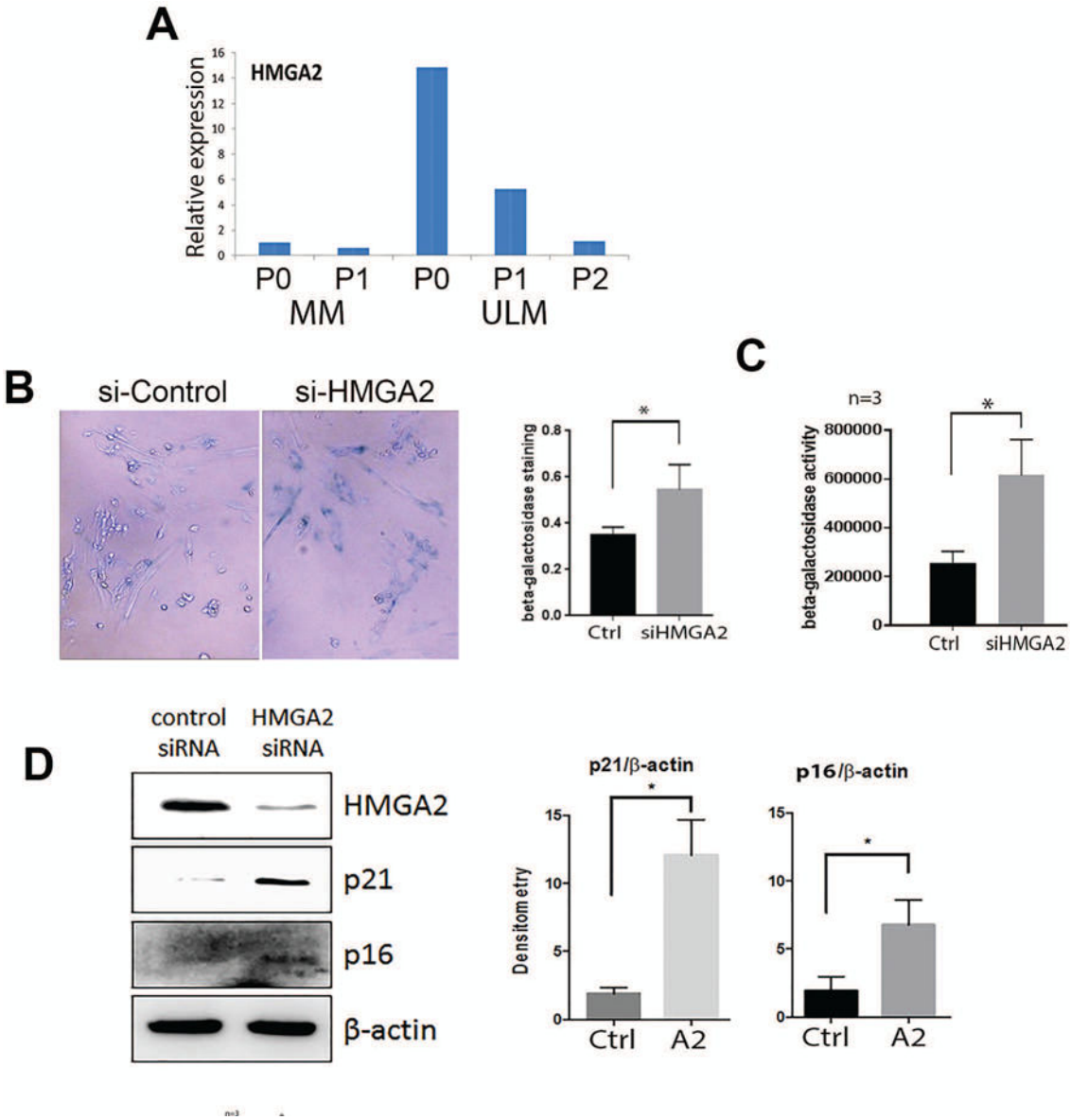

Figure 5.

HMGA2 and cellular senescence in primary ULM cells. A. *HMGA2* expression by real-time RT-PCR in myometrial (MM) and leiomyoma (ULM) cells in P0 (not passaged), P1 (passage 1) and P2 (passage 2) cultures. B. β-galactosidase staining of senescent primary leiomyoma cells after silencing of *HMGA2* by siRNA. C. Senescence in primary leiomyoma cells with silencing of *HMGA2* by siRNA measured by β-galactosidase activity. D. Repression of HMGA2 expression by siRNA increases p21 and p16 expression. Histobar panels illustrate the relative expression and significant differences between controls (Ctrl) and HMGA siRNA (A2) and MK2206 (MK) after normalized either total AKT or β-actin.

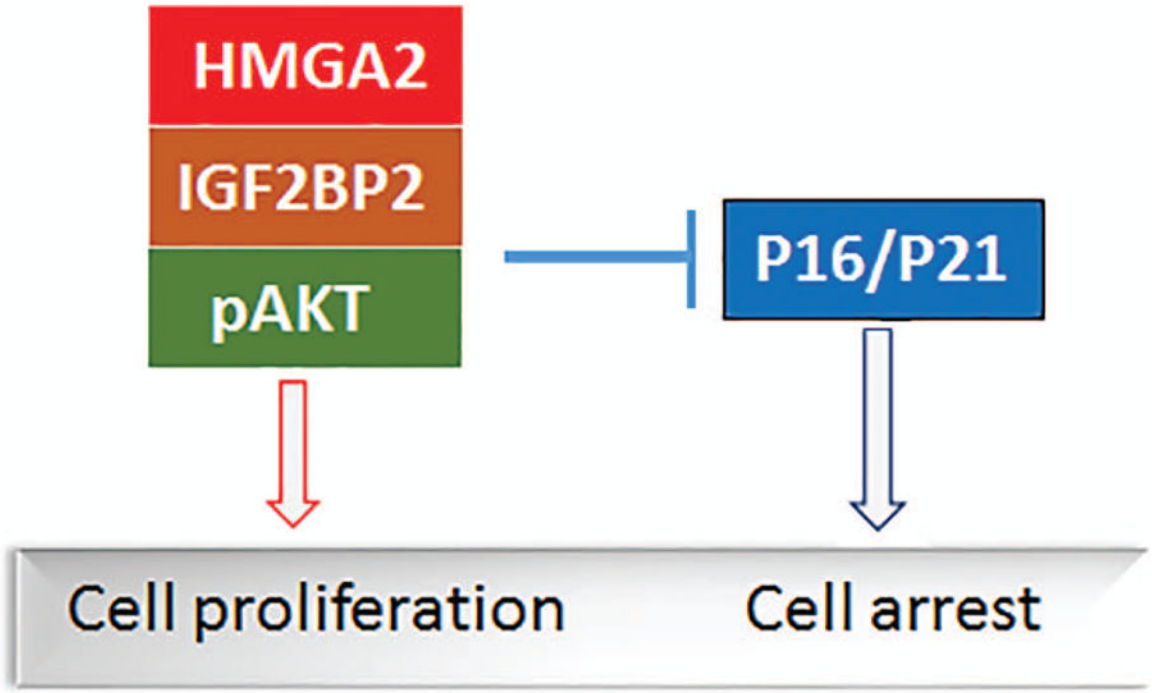

Figure 6.
Proposed model of *HMGA2* regulating AKT signaling and cell cycle genes leading to cell fate in leiomyoma cells.

Table 1

Patient demographics

		MED12	*HMGA2*	*FH*	p-value*
No. Cases		25	15	27	0.0213
Age (years)	Mean±sem**	46.1±6.2	45.6±5.7	37.7±1.7	0.0191
Tumor size (cm)	Mean±sem	6.7±0.8	11.2±2.4	8.5±0.8	

* One way Anova analysis.

** sem: standard error of the mean

Table 2

IHC expression analysis of selected genes among three molecular subtypes of ULM

		***MED12* ULM**	***HMGA2* ULM**	***FH* ULM**	**MM Controls**	**p-value***
No. cases		**25**	**15**	**27**	**40**	
ER-%	Median (low-high 95% CI)	60 (50.4–60.9)	80.0 (62.8–85.2)	45.0 (29.8–55.5)	70.0 (58.1–74.0)	0.0007
ER-I	Median (low-high 95% CI)	2.0 (1.76–2.24)	3.0 (2.11–2.82)	1.0 (0.61–1.30)	2.0 (1.88–2.43)	0.0001
PR-%	Median (low-high 95% CI)	70.0 (51.2–71.2)	80.0 (56.3–81.0)	90.0 (73.9–89.9)	75.0 (66.0–78.0)	0.0056
PR-I	Median (low-high 95% CI)	2.0 (1.84–2.56)	3.0 (2.18–2.89)	3.0 (2.59–3.03)	2.0 (2.04–2.46)	0.0044
IGF2BP2-I	Median (low-high 95% CI)	1.0 (0.31–0.92	3.0 (1.99–2.81)	1.0 (0.72—1.28)	1.0 (0.58–0.92)	0.0001
pAKT-I	Median (low-high 95% CI)	1.0 (1.20–1.66)	3.0 (2.25–2.95)	1.0 (1.26–1.67)	2.0 (1.48–1.92)	0.0001
pS6-I	Median (low-high 95% CI)	1.0 (1.23–1.68)	3.0 (2.32–2.88)	2.0 (1.35–1.77)	2.0 (1.37–1.84)	0.0001
Ki-67-%	Median (low-high 95% CI)	2.0 (1.98–4.50)	10.0 (5.56–14.04)	1.0 (0.23–2.37)	1.0 (0.57–2.01)	0.0001
P16-%	Median (low-high 95% CI)	5.0 (4.47–12.25)	1.0 (0.01–3.09)	5.0 (4.90–17.10)	1.0 (0.65–2.84)	0.0060

* One way Anova analysis.